Fracture Mechanics of Concrete Structures, de Borst et al (eds) © 2001 Swets & Zeitlinger, Lisse, ISBN 90 2651 825 0

Cable loaded uniaxial tensile tests on quasi-brittle material

C.Shi & J.G.M.van Mier
Microlab, Falculty of Civil Engineering and Geosciences, Delft University of Technology, Netherlands

ABSTRACT: Uniaxial tensile tests have been performed on single-edge-notched sandstone specimens. The specimens were loaded between cables to minimize restraint. The cable length was varied in order to study the effect of the stiffness of the test set-up. The tests were conducted under deformation control. Three types of control method were tested to investigate the effect of control system. A long distance microscope was employed to trace crack propagation and the location of crack tip. The results show that both the cable length and control method affect the crack stability. A newly developed control system based on the maximum deformation rate of the control LVDTs shows to be most successful to obtain stable test results. The advantage of the cable test is that the loading situation is clearly defined. With known location of the crack tip, high accuracy inverse analysis of softening properties becomes possible.

1 INTRODUCTION

The uniaxial tensile test is considered to be the most objective test for determining tensile parameters that are needed as input in modeling fracture in quasi-brittle materials. The measurement of tension softening behavior often requires a single crack stably propagating through the specimen. In order to maintain stability after the peak load the tests can be controlled by LVDTs and the PID settings of the regulation amplifier. However, despite the feed back system, instability appears to occur frequently, like sudden load drop and snap-back in load-deformation diagrams. Crack stability in an experiment can be affected by several factors as composition of material, stiffness of test set-up, response of control system, boundary condition, loading rate, specimen size and measuring length of the control LVDT. Some attempts have been made to investigate the stability problems in a test of quasi-brittle material, such as the work done by Van Mier & Schlangen (1989), Zhou (1989), Tandon et al (1995) etc. However, the subject is still far from being well understood.

Freely rotating boundary conditions provide a clear loading condition for a specimen and allow for the propagation of a single crack. The previous research by Van Mier (1997) and Cattaneo et al. (1999) show that flexure of hinged specimens has been identified as an important aspect of their post-peak failure behavior. However, it is difficult to make perfect hinges and often some small constraint will be imposed in one or more directions. Since this constraint is fundamentally unknown it can be difficult to reproduce experimental results by means of fracture mechanics analysis. In the present research, to further reduce the effects of constraints, cable supports have been developed and tested.

The objective of the study is to obtain a better understanding in the causes of instability in uniaxial tensile tests on quasi-brittle materials. Two series of tensile tests have been performed on single-edge-notched sandstone specimens that were loaded between cables. In one series, four different cable lengths were tested, which represent different stiffness of a test set-up. In the other series, three types of control method were used to investigate the effect of control system. A number of phenomena observed in the tests are presented in this paper.

2 EXPERIMENTAL DESCRIPTION

2.1 *Preparation of sandstone specimens*

Yellow Felser sandstone was used to produce the specimens. This type of sandstone consists of clay matrix and aggregate particles (mostly quartz and feldspar) with size of 0.05 ~ 0.7 mm, see Visser (1998). All the specimens were sawn from one large block in the same direction. The size of the specimen is 90 x 45 x 10 mm, as shown in Figure 1. The width of the specimen is chosen as 45 mm to assure that the area where a crack is expected to develop could be fully covered with a long distance

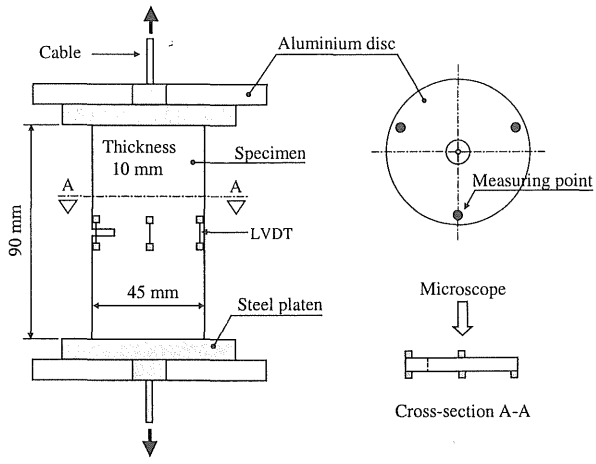

Figure 1. Arrangement of sandstone specimen.

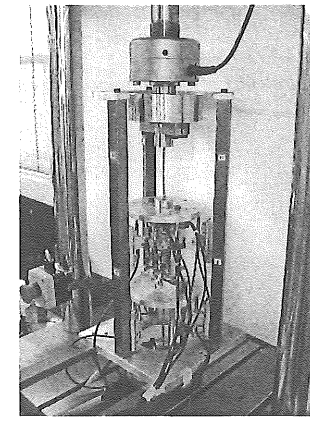

Figure 2. Set-up for cable tensile tests.

microscope. The thickness is taken small in order to avoid three-dimensional effects as much as possible. This allowed viewing only one side of the specimen with the microscope. A single 5 mm deep and 2 mm wide notch was sawn for initiating a crack. After sawing, the specimens were stored in the lab for more than 6 weeks in order to obtain constant moisture content. Furthermore, in order to improve visibility of the crack under the long distance microscope, the surfaces of the specimens were brightly painted before testing.

2.2 *Set-up for cable tensile tests*

The uniaxial tensile tests have been conducted in a servo-controlled hydraulic test machine (10 kN Instron 8872) as shown in figure 2. A specimen was glued on rectangular platens and loaded between two cables in order to eliminate boundary effects as much as possible, and to allow for the propagation of a single crack. The cable is made of steel wires and consists of 7 groups of 19 twisted wires (without ropes in between). In one series of test (test type C), four different cable lengths were used to investigate the effect of the stiffness of the set-up on the stability of crack propagation. The selected cable lengths are 200 mm, 150 mm, 100 mm and 50 mm, respectively. In another series of test (test type D) three different control methods were tested in order to study the effect on crack stability. Three to five LVDTs were mounted on the specimen to measure the deformation in the middle region of a specimen where a crack is expected to develop, see Figure 1. The vertical measuring length is 15 mm. When five LVDTs were used, three of them were positioned on the rear face and two on the front face (microscope side) of the specimen to allow the microscope to follow the crack tip till the final stage.

In addition, the vertical displacements of the top platen and bottom platen were measured in order to observe the rotation of the platens during crack propagation. For this purpose, two aluminum discs were connected to the rectangular specimen platens to provide for a sufficiently large measuring area. Three LVDTs are pointed to the upper disc and another three pointed to the bottom disc. A special frame (separated from the loading frame) has been built to mount these six LVDTs.

In order to trace the crack propagation and location of the crack tip, a long distance optical microscope (Questar, QM100 MK-III) is employed in combination with a CCD camera. Under a selected magnification, an image with a resolution of 768 x 512 pixels can be obtained. In the present tests this represents an area of 2.650 x 1.825 mm on a specimen. The largest area that can be viewed by the microscope is approximately 40 x 40 mm. A detailed description of the Questar remote measuring system can be found in Vervuurt (1997).

A newly developed control system was applied in the study, which is based on the maximum deformation rate. For this control method, more details will be given in the following section. In addition, in the test series D, two other control methods were tested in order to compare with the new control method. These two control methods are: (1) Control signal was the average of the two LVDTs close to notch; (2) Control signal was the average of four LVDTs mounted at the four corners of both notch side and non-notch side. In test series D, the cable length used was 100 mm. The rest of the conditions are all the same as in test series C.

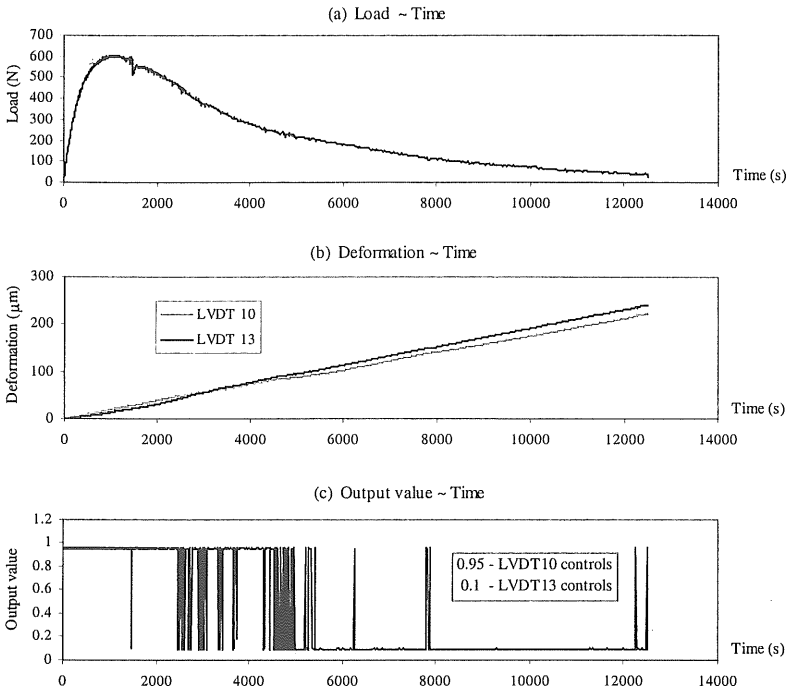

Figure 3. Control system based on deformation rate.

2.3 *A new control system*

The control method plays an important role in the whole loading procedure to obtain a stable test. In earlier tests done by Van Vliet (1999), the maximum deformation at any time, selected from a limited number of LVDTs that were fixed to a specimen, was used as control variable. This system allowed for stable crack propagation studies in large sandstone and concrete specimens (up to 2400 mm long). Drawback was that manual adjustment of the PID settings was needed with decreasing stiffness of a fracturing specimen. In the present study, a new control system has been developed in which the system continuously compares the deformation rates of the two LVDTs close to the notch. Either of these LVDTs is active. The inactive LVDT will become active whenever its deformation rate is larger than that of the active LVDT plus some threshold value. Figure 3 gives an example to show how this system controls the loading procedure. In the deformation–time diagram (Figure 3b), LVDT 10 and LVDT 13 are the controlling LVDTs mounted next to the notch. LVDT 13 is at the front side of the specimen (microscope side) and LVDT 10 is at its rear side. Figure 3(c) shows which control signal is active at a specific moment in time. When the output value is 0.95 the LVDT 10 provides the control signal and when the output value is 0.1 the LVDT 13 provides the control signal. The test results showed that this control system gives a stable tensile test and it is even capable to handle snap-back behavior.

3 PROPERTIES OF THE TEST SET-UP

3.1 *Stiffness of cables*

In order to get some idea how the cables and platens behave when they are subjected to loading and unloading under tension, a group of tests have been conducted with cable-platen sets as shown in Figure 4. These cable-platen sets are the original sets as used in the sandstone tests. All four cable lengths (200, 150, 100 and 50 mm) were tested. The tests were conducted under load control. Two specimen platens were glued together which connected with upper and lower cables so that the complete cable-platen set could be tested. Six LVDTs were mounted to measure the deformation of cable-platen set.

For every set of cable length, pre-tension of 1.5 kN (which is about 2 ~ 3 times higher than the peak-load of sandstone specimens) was applied in order to strengthen the connection between cables and platens. In subsequent tests, load path was chosen as illustrated in Figure 5. Load rate was selected as 1 N/s, which is the slowest loading speed from the

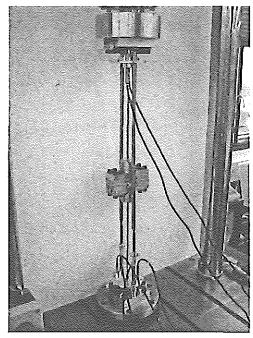

Figure 4. Set-up for the tests of cable-platen stiffness.

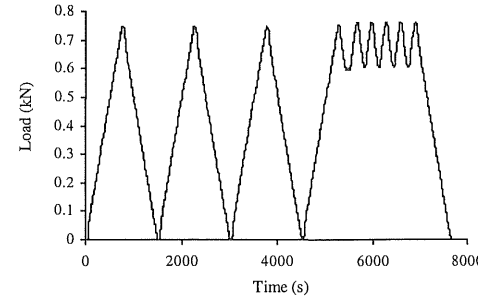

Figure 5. Load path for determining the stiffness of cable-platen system .

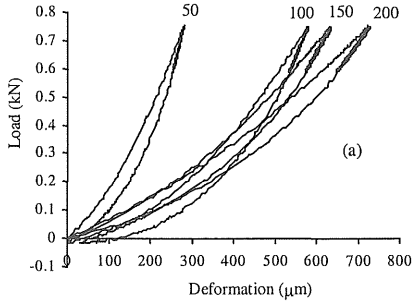

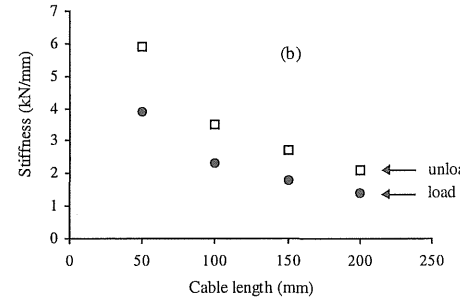

Figure 6. Results of stiffness tests: (a) Load-deformation diagrams, (b) Stiffness of the cable-platen system around peak-load for different cable lengths.

machine and is closest to the initial slope of softening curve of a sandstone specimen. The maximum load was set to 0.75 kN (around peak-load of sandstone specimens). Firstly three complete loading cycles were performed. In the subsequent loading, five small cycles were performed around peak-load with a cycle range of 0.15 kN. Since in the normal sandstone tests, the interval between the subsequent two tests was one day or longer, the same tests were performed again in one or two days after the first loading sequence. The results show that the cable stiffness can be recovered almost completely after one day. Some representative results from the stiffness tests are shown in Figure 6.

The load-deformation diagrams (Figure 6a) show that the cable-platen sets behave nonlinearly during loading and unloading, except for the regime around peak-load. The explanation is that the external loading creates friction among the twisted wires in the cable. For the complete loading cycle (load till peak-load then unload till zero), loading and unloading curves follow different paths. Around the peak-load, the unloading stiffness is about 1.5 times the loading stiffness (see Figure 6b). This higher unloading stiffness might be benefit to tension tests of softening materials because higher unloading stiffness provides quicker reaction whenever a crack opens too fast. For different cable lengths, just as expected, the longer the cable, the lower the stiffness. The results of small loading cycles show that after the first unloading, the reloading and unloading stiffness become almost identical, both follow the unloading path (higher stiffness). In the softening regime of sandstone, small load drops occur frequently and this property of the cable seems to give an improvement of the system reaction time.

3.2 *Rotation capability of specimen platens*

In the test series C, four cable lengths have been tested. Displacements of the upper and lower specimen platens were measured by means of two attached aluminium discs that provide a measuring area (see Figure 1). From the measuring data, the rotation angles of the platens during the whole loading procedure can be calculated. Figure 7 presents the diagrams of rotation angles versus time, corresponding to four different cable lengths. In the figure, the regions above and below the time-axis represent the rotation of the top platen and the bottom platen respectively.

The results show that the rotation angles of the platen increase approximately linearly, except the larger deviation in the case of 50 mm cable length.

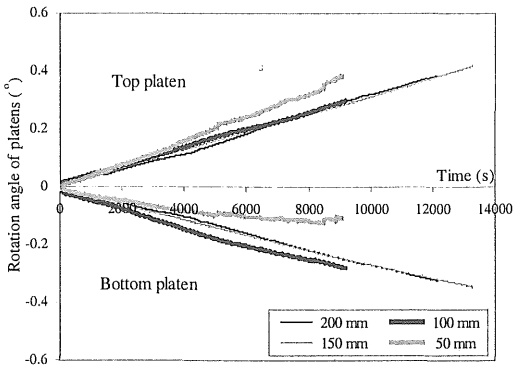

Figure 7. Rotation of loading platens for the tested four cable lengths.

The eccentric rotation of the top and bottom platens resulted from non-symmetric crack propagation. In general, for the tests with longer cable (L = 200 or 150 mm), a larger free rotation of the platens was observed, and correspondingly, larger crack opening was obtained. It seems that the shorter cable provides some constraint to prevent the platens to rotate freely. Compared to the longer cable tests, there was very little chance for shorter cable tests (L = 50 mm) to exceed a deformation of 200 μm. The lower rotation capability of the platens might be part of the cause to induce the test to fail earlier.

In addition, it is observed that the rotation angle of the platens is larger than the rotation angle of the crack faces. Part of the platen rotation must be caused by the bending and elastic unloading of the parts of the specimen outside the crack zone.

3.3 *Horizontal displacement of cables*

When a specimen is tension loaded through cables, theoretically no horizontal displacement will occur during crack opening. However, considering imperfections in the test set-up, it was felt that this should be checked. Therefore, a number of tensile tests was conducted in which the horizontal displacements of the cables were measured.

The longest cable (200 mm) was selected, which may show the most significant horizontal displacement. The horizontal displacements at the top of the lower cable were measured in-plane and out-of-plane of the specimen by means of two LVDTs. To distinguish between systematic errors and the real horizontal displacement of the cable, tests have been performed by loading both sandstone specimens (including cracking) and an aluminium specimen (deforming elastically without cracking). The results are shown in Figure 8 and Table 1.

The results of the sandstone tests show that the measured horizontal displacements of the lower

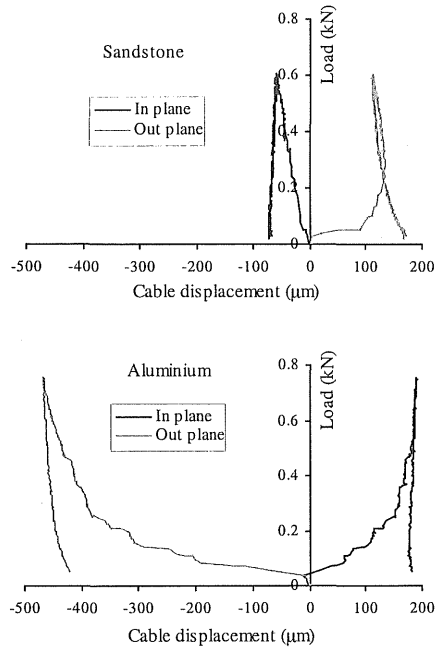

Figure 8. Load versus horizontal cable displacements from aluminium and sandstone tests.

Table 1. Horizontal displacements of the cable obtained from tests in aluminium and sandstone specimens

Specimen	Test No.	Displacement of cable	
		In-plane	Out-plane
		μm	μm
Aluminium	Cable02	183.3	------
	Cable03	196.7	449.4
Sandstone	SS11	50.0	162.1
	SS13	73.4	171.3

cable are much smaller than in the aluminium tests. This indicates that the opening of a crack in the specimen does not introduce a horizontal displacement of the cables. The measured displacements, mostly shown in the pre-peak regime, are due to the elongation and rotation of the cable under tensioning. Therefore, in the subsequent experiments and data interpretation, it is assumed that the external load is properly aligned during the whole loading process. In other words, when the location of crack tip can be determined, the loading eccentricity of the intact ligament is exactly known.

4 DISCUSSION ON EXPERIMENTAL RESULTS

4.1 *Effect of cable length*

To investigate the effect of the cable length on stability of crack propagation, a series of 37 tests has

been performed with cable length of 200 mm, 150 mm, 100 mm and 50 mm respectively. In these tests, the specimens were loaded in uniaxial tension under a constant loading rate of 0.02 μm/s until a sudden failure occurred. The following shows typical results obtained from the successful tests.

4.1.1 *Crack propagation*

For all the tests, load-deformation diagrams were recorded, which show that the shapes of the curves are not visibly affected by the cable length. By means of a remotely controlled long distance microscope, the crack path was followed during the whole loading procedure. The location of the crack tip was recorded under the selected magnification of the microscope. In most of the tests the cracks initiated at the notch and propagated straight through the middle area of the specimens, as shown in Figure 9. In the figure, the image has been enhanced to make the crack better visible. No correlation between the crack pattern and the cable length was observed. When the maximum deformation measured near the notch is approximately 150 μm, the crack propagation speed slows down gradually. Furthermore, when the deformation reaches about 200 μm, the crack opening continues to increase, but the crack tip appears to stop almost completely. Apparently, at this stage the stiffness of the intact segment becomes very low, and the eccentricity is large. Bending dominates the specimen behavior. The two segments of the specimen beyond the crack mainly rotate around the center of the intact area.

Representative load-deformation diagrams for the tests using four different cable lengths are presented in Figure 10 (a) to (d). In these figures, δ is the average of the deformations measured by the two LVDTs close to the notch. Note that the test was controlled by means of the deformation rate of one of these LVDTs as described in section 2.3.

In general, it appears that the longer cables (200 and 150 mm) give a more stable crack propagation and larger crack opening at failure than the shorter ones (100 and 50 mm). This could be explained from the (small) flexural stiffness of the cables. Particularly the short cables have some flexural stiffness and provide some constraint.

4.1.2 *Crack instability*

Local instabilities are visible in a load-deformation diagram as small dips. Tests with longer cables appeared to contain more instabilities than tests with the shorter cables (Figure 10). Evidently, in the longer cables more energy is stored which makes the set-up less sensitive to corrections of the control system. The control system first attempts small corrections but when these show to have little effect it will over-react and reduce the force strongly, producing a dip. In all tests the tail parts of the

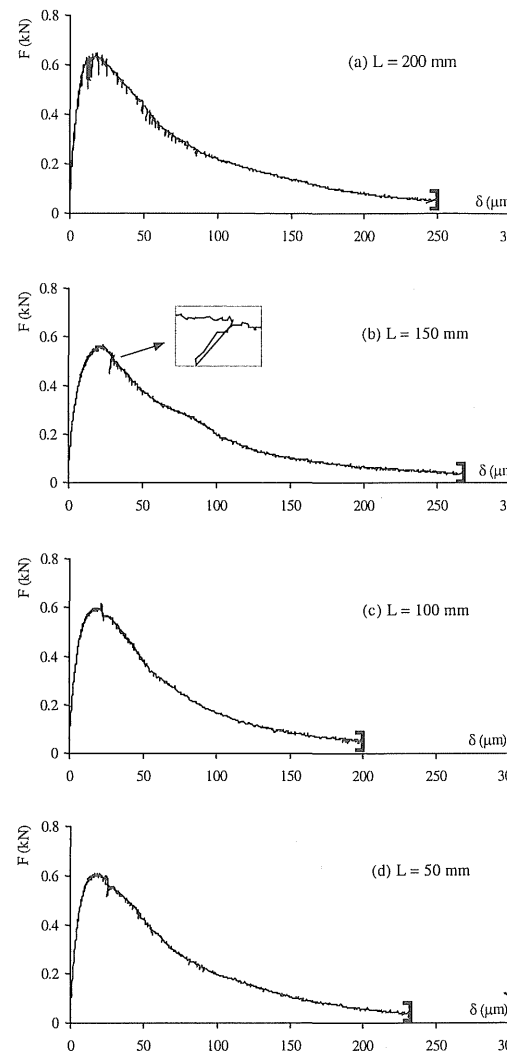

Figure 10. Load-deformation diagrams for four different cable lengths and an example of enlarged instability (snap-back) shown in the inset.

Figure 9. Example of a crack pattern from a uniaxial tensile test.

curves show to be smoother than the rest of the diagram. The reason is that at this stage the residual stiffness of the specimen becomes small due to the development of the crack, the stiffness of the cables does not dominate the control system any longer. The current control system therefore was considered an improvement to an earlier control system based on the maximum deformation in specimens

A common feature of all load-deformation curves is that substantial drops are present around the peak-load. This indicates that the system experiences considerable changes at this stage. Just before the main crack formed, the biggest amount of strain energy is stored in the system of specimen and cables, which requires a faster control system to react to sudden changes. When a crack is initiated a qualitative change occurs in the specimen. A big amount of energy releases suddenly at a high rate, and the system must be fast enough to follow the correction of the control system.

Another distinct point showing instability is at the final stage just before failure. This behavior is possibly dominated by the secondary bending moment formed in the intact area in front of the crack tip due to gradually increased load eccentricity during crack propagation. In a uniaxial tensile test between cables, the stress distribution at the cross section of a crack can be schematized as shown in Figure 11 (a) and (b) for subsequent stages of crack propagation. The stress at the crack tip is assumed to be equal to the tensile strength according to the fictitious crack model (Hillerborg (1976)). Stress in the intact area in front of the visible crack tip is distributed linearly, whereas in the area behind the crack tip, the stress distribution follows softening behavior of the material.

As the location of the applied force in the cable is exactly known (hardly any horizontal displacement of the loading cables was observed) and the location of the crack tip at failure is known to some accuracy, the test can be used for extracting softening data of the material to a high degree of accuracy. At present

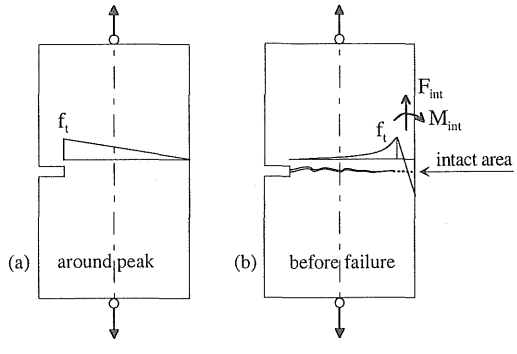

Figure 11. Stress distribution at different crack stages.

the analysis is in progress. As a result of the eccentric loading on the cracked specimen (Figure 11b) the area in front of the visible crack tip is loaded by the force F_{int} and the bending moment M_{int}. This situation will be used to assess the conditions just before final catastrophic failure.

4.2 *Effect of control method*

To investigate the effect of control method on crack stability and compare with the tests controlled by deformation rate, another group of tension test (test type D) has been performed with two other control methods: (1) average of the two LVDTs close to the notch (AV2), and (2) average of four LVDTs mounted at four corners of the specimen (AV4).

Figure 12 and 13 show typical results of control signal and load-deformation diagrams obtained from the tests controlled by AV2 and AV4. For the convenience of comparison with the test results controlled by deformation rate, the axis scale in Figure 12b and 13b are set the same as in Figure 10. The deformation δ in the figures represents the average value of the two LVDTs close to the notch. Comparing the control methods of AV2 and AV4 with deformation rate control, a few distinct features can be observed. In general, all the tree types of control methods give the same shape of curve. However, the deformation rate control provided larger stable crack propagation than the other two control methods. On average, tests controlled by deformation rate can reach a maximum deformation higher than 200 μm. Totally 7 tests were conducted under AV2 control. The maximum deformations were all smaller than 140 μm. In the 3 tests controlled by AV4, only one reached 200 μm, the two others failed before 140 μm deformation. Under the same loading rate, the crack propagated much faster in the tests controlled by AV4. This is due to the large difference between control signal and the deformation measured by the individual LVDTs.

In addition, Control methods of AV2 and AV4 showed that they were insensitive to out-of-plane bending of the specimen, see Figure 12a and 13a. Furthermore, in the tests controlled by AV2 and AV4, periodic fluctuations occurred in the post peak regime. More pronounced fluctuations were observed in the AV4 tests. The local vibration appears to be larger than in deformation rate controlled tests for the same cable length (100 mm). The same phenomenon was found in tests with 200 mm cable length, controlled by deformation rate. This indicates that the AV2 and AV4 methods provide a slower reaction than deformation rate control for the same cable length.

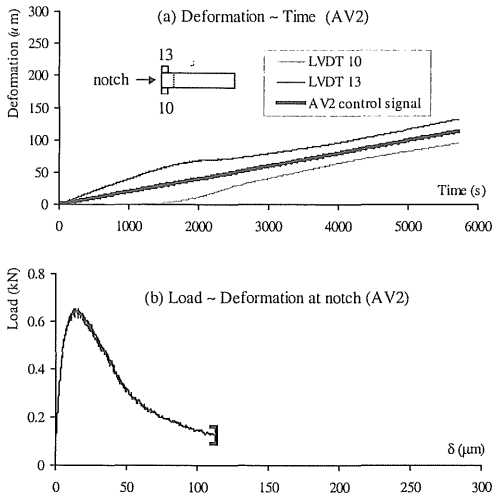

Figure 12. Control signal and load-deformation diagram from a test controlled by AV2.

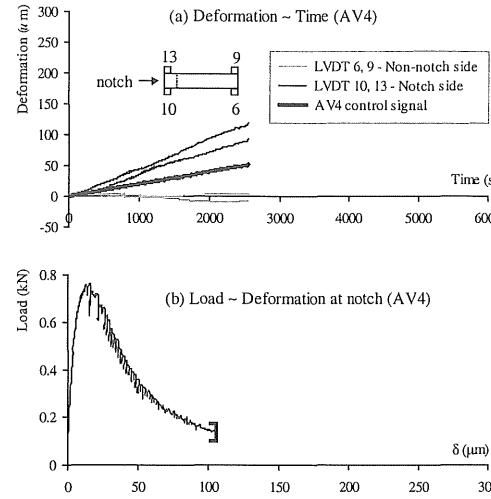

Figure 13. Control signal and load-deformation diagram from a test controlled by AV4.

5 CONCLUSIONS

Two series of sandstone tensile test have been conducted in which the specimens were loaded through cables. Both the stiffness of the test set-up (represented by a variation of the cable length) and control method affect stability of crack propagation.

The newly developed control system, which is based on the rate of crack opening at the notch tip, is very well suited for obtaining stable load-deformation diagrams under uniaxial tension irrespective of the machine stiffness.

The tests showed local instabilities, which were successfully handled by the control system except for the catastrophic failure at large crack openings.

The loading situation in the specimen is very clear. The point of load application is well defined, and since the tip of the crack is known to some accuracy, inverse analysis of tension softening properties of the tested material is possible to a high degree of accuracy, which is considered an important improvement in test technique in comparison to the fixed platen test prescribed in the first publication of the fictitious crack model. Moreover, the cables operate as hinges, and a lower bond of fracture energy is measured which is considered important for structural analysis.

6 ACKNOWLEDGEMENTS

This research was supported by Dutch Technology foundation (STW) and the Priority Program Materials Research (PPM). The authors are indebted to Allard Elgersma for his invaluable assistance in carrying out the experiments.

7 REFERENCES

Van Mier, J.G.M. & Schlangen, E. 1989. On stability of softening system. In S.P. Shah, S.E. Swartz & B. Barr (eds), *Fracture of concrete and rock – Recent developments*: 387-396. London/New York: Elsevier.

Zhou, F.P. 1989. Some aspects of tensile fracture behavior and structural response of cementitious materials. Report, Lund Institute of Technology, Sweden.

Tandon, S., Faber, K.T. & Bazant, Z.P. 1995. Crack stability in the fracture of cementitious materials. *Mat. Res. Soc. Symp. Proc.*, Vol. 370: 387-396.

Van Mier, J.G.M. 1997. *Fracture processes of concrete*, CRC Press, Boca Raton (FL).

Cattaneo, S. & Rosati, G. 1999. Effect of different boundary conditions in direct tensile tests: Experimental results. *Magaz. Concr. Res.*, vol. 51, No. 5: 365-374.

Visser, J.H.M. 1998. *Extensile hydraulic fracturing of (saturated) porous materials*. Ph.D. thesis, Delft University of Technology, Netherlands.

Vervuurt, A.H.J.M. 1997. *Interface fracture in concrete. Ph.D. thesis*. Delft University of Technology, Netherlands.

Van Vliet, M.R.A. & Van Mier, J.G.M. 1999. Effect of strain gradients on the size effect of concrete in uniaxial tension. *Int.J.Fract.*, vol 95: 195-219.

Hillerborg, A., Modeer, M. & Petersson, P.E. 1976. Analysis of crack formation and crack growth in concrete by means of fracture mechanics and finite elements. *Cem. Conc. Res.*, vol. 6: 773-782.